Available online at www.sciencedirect.com
ScienceDirect
Procedia Engineering 10 (2011) 3140–3145
Engineering Procedia
ELSEVIER

ICM11

Micro-mechanical analysis of the confined amorphous phase in semi-crystalline polymers

Pinto J.*, Castagnet S., Nadot-Martin C., Touchard F., Mellier D.

Institut P' • UPR CNRS 3346 • Département Physique et Mécanique des Matériaux
ENSMA - Téléport 2, 1er avenue Clément Ader BP 40109
F86961 FUTUROSCOPE CHASSENEUIL Cedex FRANCE

Abstract

The mechanical modelling of semi-crystalline polymers is highly complex due to their different micro-structural scales and to some lacks regarding the understanding of the respective contributions of crystalline and amorphous phases on the macroscopic behaviour. In particular, the important role of the confined amorphous phase has to be investigated. To this aim, this work proposes to combine full-field simulations with kinematics field measurements at the same scale. The material is the linear low density polyethylene (LLDPE), chosen for its "simple" microstructure. Displacement fields at the micro-scale are measured by using the digital image correlation technique in the SEM. It is scheduled to apply the experimental strain as periodic boundary conditions to a unit cell whose morphological content will be built from the observed real microstructure and to analyse both the resulting macroscopic average response and local fields. To this aim, specific numerical tools are developed notably for statistical field analysis. The results on a simple stack model under various loading cases/paths are presented as a preliminary stage before the complete analysis for the LLDPE under tensile tests.

The long term aim is to better understand the strain mechanisms in the confined amorphous phase, to determine its mechanical behaviour and conclude on its influence on the macroscopic behaviour.

Keywords: Semi-crystalline polymers, multi-scale analysis, confined amorphous phase, in situ tensile tests;

---

1. Introduction

The macro-mechanical properties of semi-crystalline polymers depend on their morphological constituents. The microstructure of semi-crystalline polymers involves the co-existence of a crystalline lamellae embedded in an amorphous phase. The behavior of the crystalline phase is known. In contrast, the behavior of the amorphous phase requires some specific complementary investigation.

Several micromechanical models have been used to describe the mechanical behavior of semi-crystalline polymers. Various approaches were made using different representations of the microstructure, like ellipsoidal crystalline inclusions in an amorphous matrix [1], aggregates of layered crystalline-amorphous planar inclusions [2], [3], [4], [5], [1], also assemblies of meso–regions, each one being an equivalent network of chains connected by

Selection and peer-review under responsibility of ICM11 doi:10.1016/j.proeng.2011.04.520

temporary junctions [6]. The amorphous phase was considered as: elastic [1], viscoplastic [2], viscoelastic [4], [6] or elasto-viscoplastic [3].

From an experimental point of view the micro-mechanical characterisation of semi-crystalline polymers presents lots of restrains due to the fine scale of the morphological constituents. One way to perform the strain measurement at the scale of the morphological constituents of these kind of materials is to use the digital image correlation (DIC) coupled with the in-situ tensile test technique in the SEM. This technique was already used by [7] to measure the in plane displacements on a Ti-6Al-4V titanium alloy surface with a subset size of about 1μm ; and more recently by [8] to study the micro-scale mechanical behaviour of a polymer-bonded explosive using the natural micro-structural features as a random speckle pattern with a subset size of about 4μm.

The amorphous phase in the semi-crystalline polymers could be defined as an assembly of disordered macromolecules. Its behaviour is usually affected by the presence of the crystalline lamellae, which restrains the deformation. The amorphous phase could be divided in two types: the inter-lamellar where the chains are typically constrained by the crystalline lamellae and the rubber like one usually located around the spherulitic structures and less conditioned by the crystalline lamellae.

As results of the different constrains implied by the crystalline phase, the amorphous one presents a heterogeneous strain evolution during the deformation. In order to better understand the deformations mechanisms inside the amorphous phase and the influence of the crystalline phase on the amorphous phase deformation, a simple stack model was first used for different loading paths and types. Different numerical tools were developed and exploited for the analysis of the simple stack model with the aim to be applied to a much more complex model.

Digital image correlation technique was enhanced to measure strain fields at the micro-scale under interest for semi-crystalline polymers.

With a better understanding of the strain heterogeneity and deformation mechanisms of the amorphous phase, we expect a better understanding of its influence on the macroscopic behaviour of the material.

2. In situ tensile tests using the digital image correlation

2.1. Material

The material used is the linear low density polyethylene (LLDPE) in granulated form. The pellets were pressed above the fusion temperature into rectangular plates with 2 mm of thickness, and then annealed at 75 °C. After this procedure the micro-samples were machined from the plates according to the geometry presented in figure 1b. In order to obtain a correct contrast between the material phases in the SEM, a surface treatment has been specially adapted to the micro-samples: a micro-polishing procedure followed by permanganic etching for 6 hours in a reagent made up of 65.8 wt% H_2SO_4, 32.9wt% H_3PO_4, 1.3 wt% $KMnO_4$ [9]. This material is chosen because it presents crystallization difficulties and consequently a simple microstructure, as observed in figure 1a, which is welcome for further reconstruction in view of finite element (FE) analysis.

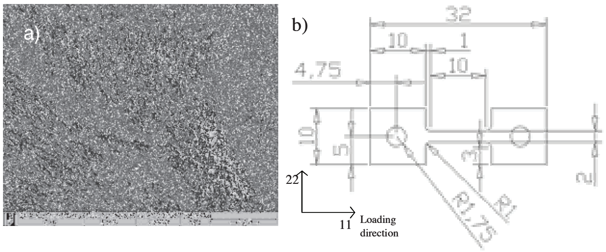

Figure 1 – LLDPE microstructure observed by SEM (a), and micro-testing specimen geometry in (mm) (b).

2.2. Method description

To measure whole-field 2D displacements, we use a method based on the comparison of two random grainy pattern images. For this kind of technique, the principle is to record the object surface twice, before and after loading. The first image is divided into small sub-windows of NxN pixels (40x40 pixels in this case). The discrete matrix of the values of pixel grey level in each sub-window forms an exclusive fingerprint identification within the image. The correlation between sub-windows in the two pictures allows the determination of the in plane displacement, caused by the deformation, at every sub-window center. With the in-plane displacement field, the data is transmitted to a FEM code ABAQUS®. This software is then used to derive from the experimental data the in-plane strain values. Several tests shown that the digital image correlation procedure developed, leads to an accuracy of displacement values of about 1/10 pixel.

In this work the DIC technique was applied at the micro-scale using the SEM, to measure the displacement fields in the LLDPE.

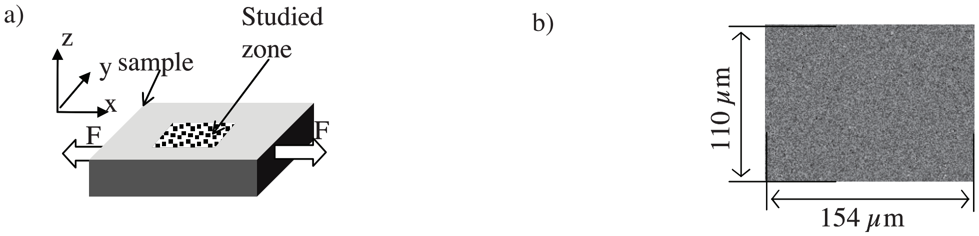

Figure 2 – Experimental set up of the in situ tensile test (a), picture of the random grainy pattern in the studied zone (b).

The used random grainy pattern (figure 2b) contains dots of approximately 165 nm size. It leads to a spatial resolution of 2.2 μm for each sub-window. As the material presents an average spherulitic diameter of about 9 μm, it is possible to have 4 sub-windows of measurement inside a spherulite.

The tensile tests were performed inside a JEOL-6100 SEM, using a monotonic tensile tests micro-machine with a 600N load cell, a maximum jaw displacement of 10 mm and a displacement rate of 0.02mm/min. At any time it was possible to stop the test and to capture a high resolution image of the random grainy pattern. The simplified experimental set up for the tensile test is shown in figure 2a.

3. Numerical simulation

3.1. Geometry

At the microscopic scale the semi-crystalline polymers are heterogeneous materials consisting the co-existence of crystalline and amorphous phases. In figure 3a it is shown the TEM observations of a HDPE microstructure, from which a simple stack model was developed as a preliminary stage of the research program.

The simple stack model is periodic with a unit cell which consists in a crystalline lamella surrounded by half of amorphous layer. Also considering the symmetry conditions, only a 1/8 of the basic cell is built. The model was analyzed using the finite element method (FEM) from ABAQUS®. The corresponding mesh using C3D8 elements is shown in figure 3b.

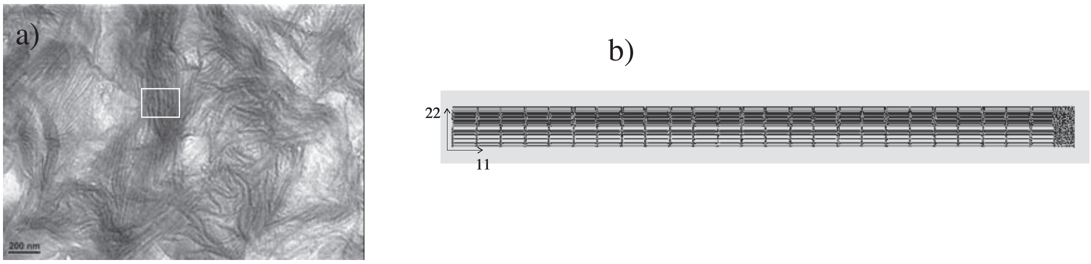

Figure 3 - TEM observation of the HDPE microstructure (a); 1/8 of the unit cell of the pack (simple stack model) for FE analysis (ABAQUS®) (b).

3.2. Mechanical Properties of the phases

The crystalline phase is considered as orthotropic linear elastic [10]. The properties are reported in table 1.

Table 1 – Material coefficients for the orthotropic elastic law of crystalline phase in the HDPE [GPa] [10].

C11	C33	C22	C13	C12	C32	C44	C55	C66
13.8	325	12.5	7.34	2.46	3.96	1.98	3.19	6.24

No distinction is here made between the inter-lamellar amorphous phase and the amorphous phase around the crystalline lamellae. It is considered as isotropic linear viscoelastic, using the Pronys series formulation available in the software ABAQUS®.

The shear and bulk modulus are distributed over ten relaxation times ranging over four decades, between 1 and 1000 seconds. The glassy Young's modulus of this reduced distribution is 300 MPa and the relaxed one is 17 MPa; this leads to a glassy and relaxed value of 100 and 94 MPa respectively for the shear modulus.

In terms of bulk relaxation modulus, it is assumed a constant Poisson ratio hypothesis.

3.3. Boundary conditions

Periodic boundary conditions are applied for the FEM analysis. These conditions are based on the equation 1.

$$\mathbf{u} - \mathbf{E}.\mathbf{y} \quad \text{periodic in } \partial \mathrm{V} \qquad (1)$$

where **E** denotes the macroscopic, average, strain tensor characterizing the loading to be applied, **u** and **y** are respectively the displacement and position vectors of any point of the boundary $\partial \mathrm{V}$. The quantity defined in Eq. (1) takes the same value at two homologous points on opposite faces of the unit cell while the traction vector $\boldsymbol{\sigma} \cdot \mathbf{n}$ takes opposite values.

Even if the model in study would allow 2D analysis with symmetry conditions, the periodic boundary conditions, Eq (1), are programmed in ABAQUS® in a 3D wide-ranging way (for further application to any complex microstructure). Indeed, in the case of random microstructures (i.e. non periodic), the periodic boundary conditions are known to be more precise than homogeneous strain or stress boundary conditions [11].

3.3.1. Loading types/paths

Three kind of loading types are studied: in plane shear and unidirectional tensile loadings along the transversal and longitudinal directions of the lamellae (22 and 11 respectively in figure 3b). These loading types allow getting closer to the real loadings that the crystalline lamellae may undergo inside of the spherulitic structure.

For each loading type, loading/unloading paths are considered with relaxation and anti-relaxation stages (2000 seconds for each). Such a complex loading path allows the study of the relaxation/antirelaxation mechanisms of the amorphous phase. The loading path with a total duration of 4800 seconds is schematized in figure 4.

The imposed strain rate is 1E-5 for the shear loading, 3E-5 and 2E-5 for the tensile loadings respectively along the transversal and longitudinal directions of the lamellae.

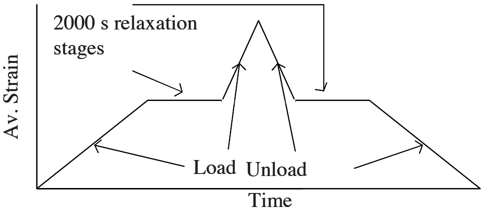

Figure 4 -Loading/unloading path with relaxation and anti-relaxation stages with a total duration of 4800 seconds.

3.4. Numerical tools for fields statistical analysis

Classical volume averages over the whole unit cell and over each phase are computed, (see e.g. [12]) as well as averages of second-order moments over the phases for a first analysis of the intraphase field fluctuations. These tools are programmed in the form of PYTHON® scripts.

For a more detailed analysis of the stress and strain field fluctuations, a probability density function is also added, as proposed by e.g. [13]. This function quantifies for the elements of a given phase the number of occurrences of a given value (for a variable z) in each class (range of values). This statistical tool is also programmed via a PYTHON® script in order to systematise the models analysis.

3.5. Results

As an illustration, the results for the shear loading are presented in figure 5a. The average stress in the amorphous phase is presented in function of the time with the respective standard deviation values. It is possible to observe that along the loading path the standard deviation grows when the stress values grow. The maximum value of standard deviation is observed for 2400 seconds. The corresponding probability density function is presented in figure 5b.

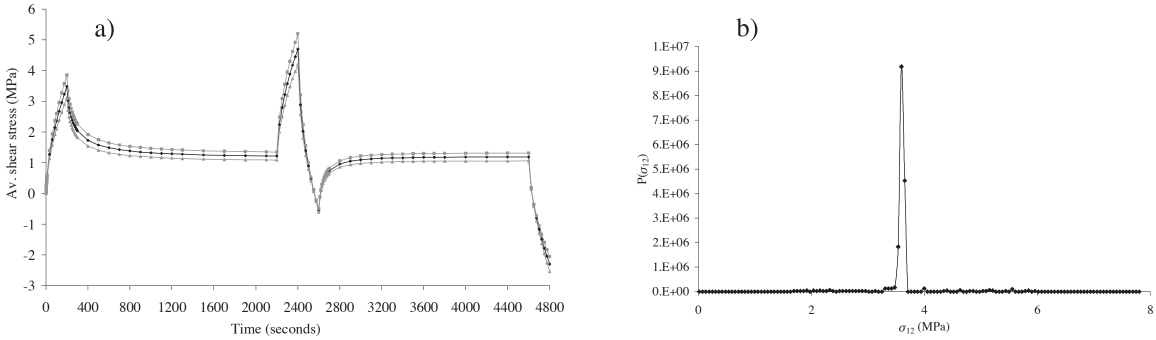

Figure 5 – Evolution of the volume average stress in the amorphous phase (a), probability density function of the shear stress for 2400 seconds (b).

The probability density function shows the existence of a single peak, which indicates that the intraphase heterogeneity is weak even for the step time where the standard deviation is the strongest.

4. Conclusion

For the context of this topic a DIC technique at the micro scale was presented. In this technique the spatial resolution obtained is thin (1 dot -165 nm), it permits strain measurements at the spherulitic scale. The average strain measured inside the studied zone is found to be near the macroscopic strain (deduced from the jaw displacement).

Numerical tools for the application of 3D periodic conditions in ABAQUS® and for the post treatment of microstructure full-field simulations were developed. Even if these tools have been first exploited for the analysis of a simple stack model, they are ready for further analysis of a more complex, representative, model currently in construction. These tools allow analyzing the evolution of the average stress and strain in the microstructure or in the constitutive phases and also to quantify their fluctuations. The coupling of fields statistical analysis (via second-order moments and probability density functions) to local maps provided by ABAQUS® software constitutes an efficient tool to quantify fields heterogeneity and further improve the understanding of the strain mechanisms in the confined amorphous phase.

Preliminary results obtained for the sample stack model show that during the relaxation stage, the variance values drops more intensively down to a stabilization regime in the shear case than in the transversal tensile one. Also the fields fluctuations are always more important for the transversal tensile loading than for the shear loading.

For further work it is scheduled to apply the measured strain (via periodic boundary conditions) to a model of the microstructure observed in the studied zone.

Acknowledgements

The authors are grateful to the help of Mr. Roland Seguela for providing the LLDPE pellets to the experimental study. The authors are also grateful to Mr. B. Arbeille, the responsible of the Laboratoire de Biologie Cellulaire – Microscopie Electronique of the Faculté de Médecine de Tours, for the utilisation of the cryo-ultramicrotome, and to Mr M. Gerland for the MET observations.

References

[1] F. Bédoui, J. Diani, G. Régnier, W. Seiler, “Micromechanical modeling of isotropic elastic behavior of semicrystalline polymers,” *Acta Materialia*, vol. 54, Avr. 2006, p. 1513-1523.

[2] B. Lee, D. Parks, S. Ahzi, “Micromechanical modeling of large plastic deformation and texture evolution in semi-crystalline polymers,” *Journal of the Mechanics Physics of Solids*, vol. 41, 1993, p. 1651-1687.

[3] J. Van Dommelen, D. Parks, M. Boyce, W. Breklemans, F. Baaijens, “Micromechanical modeling of intraspherolitic deformation os semicrystalline polymers,” *Polymer*, vol. 44, 2003, p. 6086-6101.

[4] S. Nikolov and I. Doghri, “A micro/macro constitutive model for the small-deformation of the polyethylene,” *Polymer*, vol. 41, 2000, p. 1883-1891.

[5] W. Yang and M. Chen, “Modeling of large plastic deformation crystalline polymers,” *Journal of the Mechanics and Physics of Solids*, vol. 49, 2001, p. 1719-1736.

[6] A. Drozdov and R. Gupta, “Non-linear viscoelasticity and viscoplasticity of isotatic polypropylene,” *International Journal of Engineering Science*, vol. 41, 2003.

[7] F. Lagattu-Touchard, F. Bridier, P. Villechaise, J. Brillaud, “In plane strain measurements on a microscopic scale by coupling digital image correlation and an in situ SEM technique,” *Materials Characterization*, vol. 56, 2006, p. 10-18.

[8] Z. Zhou, P. Chen, F. Huang, S. Liu, “Experimental study on themicromechanical behavior of a PBX simulant using SEM and digital image correlation method,” *Optics and Lasers in Engineering*, vol. 49, 2011, p. 366-370.

[9] F. Addiego, A. Dahoun, C. G'Sell, J. Hiver, “Characterization of volume strain at large deformation under uniaxial tension in high-density polyethylene,” *Polymer*, vol. 47, 2006, p. 4387-4399.

[10] C. Choy and W. Leung, “Elastic Moduli of Ultradrawn Polyethylene,” *Journal of Polymer Science: Polymer Physics Edition*, vol. 23, 1985, p. 1759-1780.

[11] T. Kanit, F. N'Guyen, S. Forest, D. Jeulin, M. Reed, S. Singleton, “Apparent and effective physical properties of heterogeneous materials: Representative of samples of two materials from food industry,” *Comput. Methods Appl. Mech. Engrg.*, vol. 195, 2006, p. 3960-3982.

[12] J. Michel, “Materiaux aléatoires élastiques et milieux périodiques,” *Théorie des milieux périodiques In: Homogénéisation en mécanique des materiaux 1*, Paris: HERMES Science Publications, 2001.

[13] M. Idiart, H. Moulinec, P. Ponte Castañeda, P. Suquet, “Macroscopic behaviour and field fluctuations in viscoplastic composites: Second order estimates versus full-field simulations,” *Journal of the Mechanics and Physics of Solids*, vol. 54, 2006, p. 1029-1063.